IEEE Access
Multidisciplinary | Rapid Review | Open Access Journal

Received July 9, 2019, accepted August 3, 2019, date of publication August 12, 2019, date of current version August 27, 2019.

Digital Object Identifier 10.1109/ACCESS.2019.2934641

Energy Efficiency in Multiple Antenna Machine-Type Communications With Reconfigurable RF Transceivers

EDSON LEONARDO DOS SANTOS[1], ANDRÉ AUGUSTO MARIANO[1], (Senior Member, IEEE), GLAUBER BRANTE[2], (Senior Member, IEEE), BERNARDO LEITE[1], (Member, IEEE), RICHARD DEMO SOUZA[3], (Senior Member, IEEE), AND THIERRY TARIS[4], (Member, IEEE)

[1]Federal University of Paraná (UFPR), Curitiba 81531-980, Brazil
[2]Federal University of Technology—Paraná (UTFPR), Curitiba 80230-901, Brazil
[3]Federal University of Santa Catarina (UFSC), Florianópolis 88040-900, Brazil
[4]University of Bordeaux, 33405 Talence, France

Corresponding author: Glauber Brante (gbrante@utfpr.edu.br)

This work was supported by INESC P&D Brasil. This work was developed in Project F-LOCO with Grupo Energisa, under the framework of the Research and Development (R&D) Program regulated by Agência Nacional de Energia Elétrica (ANEEL), code PD-00405-1804/2018. This study was financed in part by Coordenação de Aperfeiçoamento de Pessoal de Nível Superior (CAPES), Finance Code 001, PrInt CAPES-UFSC "Automation 4.0," and by the National Council for Scientific and Technological Development (CNPq) Brazil.

ABSTRACT In machine-type communication (MTC) networks, each node is equipped with a set of radio-frequency (RF) transceivers, antennas and power source. Besides, wireless nodes are typically battery-powered, whose recharging or replacement is often not viable or even impossible. Therefore, in such systems where energy is at a premium, minimizing power consumption improves energy efficiency and increases battery lifetime. In this paper, a novel energy-saving approach includes in the communication system model the use of reconfigurable RF transceivers. More specifically, the components involved in our power minimization framework are the power amplifier (PA) at the transmitter and the low noise amplifier (LNA) at the receiver, which are the blocks responsible for RF amplification and are on top of power consuming blocks in RF transceivers. Our goal is to show that RF circuits based on multimode operation can significantly improve the energy efficiency. We perform a joint selection of the best operating modes for PA and LNA circuits in different communication scenarios. Results show that by combining PA and LNA operating modes, an improvement of more than 75% in energy efficiency is obtained for multiple antenna communications, when compared to the state-of-the-art literature of non-reconfigurable amplifiers. Besides, we show that adapting spectral efficiency contributes towards improving energy efficiency. In this case, we consider different spectral efficiency values, including the effect that the PA operates at different backed-off power levels. In addition, when comparing single-input single-output (SISO) and multiple-input multiple-output (MIMO) transmission schemes, antenna selection (AS) outperforms the others schemes in terms of energy efficiency for short and moderate distances, but singular value decomposition (SVD) allows for longer communication distances.

INDEX TERMS Energy efficiency, reconfigurable RF transceivers, machine-type communications, multiple antennas.

I. INTRODUCTION

Low-power, low-size and low-cost implementations are essential in several applications for sensing, monitoring and control, of which machine-type communication (MTC) scenarios typically consist. MTC networks are one of the most important use-cases of 5G communication systems and a building block of the Industry 4.0 paradigm [1]–[3], where not only sensors, but also other types of devices communicate without the need of human interaction. In fact, the number of connected devices is expected to be substantially large in wireless networks, 50 billion connected devices by 2020 according to [4]. Such massive collection of devices will have great challenges in terms of connectivity, reconfigurability

The associate editor coordinating the review of this article and approving it for publication was Javed Iqbal.

and energy efficiency. In particular, since wireless nodes will be mainly powered by batteries, or even by solar cells that can seldom or never be recharged, one of the most noteworthy concerns is the efficient use of limited power sources [5].

Another challenge found in MTC networks is the wireless environment itself. Due to channel fading, high transmit power is usually required for reliable communications [6], which compromises the energy efficiency of MTC networks. A possible candidate to reduce the power required to transmit is to employ more antennas [6]. A multiple-input multiple-output (MIMO) arrangement exploits spatial diversity gains in order to improve the link reliability, allowing wireless nodes to transmit with reduced power. It is worth noting that great advances in the design of antenna arrangements have been reached in recent years [7], [8], making the use of multiple antennas on small nodes possible. Nevertheless, a key element that must be taken into account is the power consumption of the radio-frequency (RF) transceiver circuits. Although MIMO can considerably improve the signal-to-noise ratio (SNR) when compared to the transmission with a single antenna, multiple antennas also implies in multiple RF chains, consuming more power at the circuit level [9].

RF transceivers are typically designed considering the 'worst-case' scenario in compliance with a standard and, consequently, present a fixed operating point. However, high performance is not always required during system operation, so that electronic circuits are often over-specified. Thereby, in situations where the communication link is better than the worst-case assumption, circuits end up consuming more power than necessary. For this reason, we can change the circuit operating point, i.e., reduce the performance without prejudice to the target communication, and thus save energy. In this way, the use of reconfigurable circuits is seen as a possible solution to acquire greater energy autonomy, in which the trade-off between higher performance and lower consumption can be adjusted according to the communication scenario [10]. Therefore, the design of power-efficient reconfigurable RF transceivers combined with the spatial diversity benefit of using multiple antennas has become a key aspect in extending the lifetime of wireless devices [11].

In this paper, we analyze the energy efficiency in MTC scenarios. In contrast to much of the available literature, our energy-saving approach includes reconfigurable RF transceivers. We consider the circuits of the power amplifier (PA) and the low noise amplifier (LNA), exploiting different operating modes that impact the power consumption, while the other circuits of the RF chain have only one operating mode. We employ state-of-the-art circuits, using real data from the reconfigurable PA proposed by [12] and the reconfigurable LNA in [13]. Furthermore, for better positioning the contribution of this paper, we compare the results with those of two state-of-the-art non-reconfigurable circuits designed for high performance, the PA proposed by [14] and the LNA in [15]. We further assume a MIMO design, which allows us to combine the reconfigurable capability of the transceiver circuits with spatial diversity transmission schemes. In particular, we consider an antenna selection (AS) scheme, in which a single pair of antennas is used between the transmitter and receiver to reduce the power consumption, and a MIMO beamforming scheme based on singular value decomposition (SVD), which uses all transmit and receive antennas concurrently to improve reliability. A single-input single-output (SISO) scheme is also considered for comparison. Aiming at maximizing the energy efficiency of the communication system, we perform a joint selection of the best operating modes for the PA and the LNA, as well as adapting the spectral efficiency, given a quality of service (QoS) constraint in the receiver, expressed in terms of a maximal allowed outage probability.

A. RELATED WORK

At the transmitter, the PA is responsible for amplifying the signal to be emitted by the antenna and is the block with the highest power consumption [16]. Therefore, the optimal tuning of the PA parameters is crucial for achieving high energy efficiency. In the design of a PA, metrics such as power gain, output power, stability, linearity and efficiency are usually the most important parameters. However, it is not possible to maximize all these metrics at the same time, and thus most designs focus on a trade-off between some of these parameters. Aiming at minimizing the PA power consumption, reducing the power gain or the output power is usually employed in order to create other operating modes with lower consumption. For instance, the authors in [17] provide different current levels by turning off parts of the circuit, with a difference as high as 50% in terms of power consumption between low-power and high-power modes. In addition, by controlling the supply voltage levels of the transistors, works such as in [18], [19] also create low-power modes that can reduce up to 650 mA in the direct current consumption. Yet, the discrete resizing of amplifier structures is employed in [20] with a similar goal, reducing the direct current from 590 mA to 105 mA in the low-power mode.

Besides creating low-power modes, another common practice to reach reconfigurability is to implement multi-stage architectures. For example, the PA proposed in [21] consists of two stages, the first allowing variable power gain and the second with fixed output power. Such design provides a range of operating modes between low-gain and high-gain modes. The work in [21] has been recently extended in order to consider both stages being reconfigurable [12]. Such combination is controlled by six digital switches, three at each stage, yielding 64 possible operating modes with different gains, power levels, linearity and power consumption. The PA in [12] admits the power gain to vary from 18 dB to 31 dB, the output 1 dB compression point varies from 7.5 dBm to 16.9 dBm, whereas the power consumption can be as low as 153 mW, up to 394 mW in high-power modes. This PA provides significant reconfigurability for the 2.4 GHz band.

Furthermore, the design of reconfigurable PAs may improve efficiency under modulated signals, which typically

have a high peak-to-average power ratio (PAPR) and limit the average output power of the transmitter device. A graceful power back-off is demonstrated in [22], where a combination of source and load modulation is proposed for larger efficiency improvements at low output power over high PAPR signals. Measurement results show an efficiency of the PA of up to 44% at 13 dBm with 7.4 dB PAPR.

At the receiver, the LNA, located after the antenna is responsible for the sensitivity of the receiver through its noise factor [23]. Its function is to amplify the received signal with minimal distortion. Thus, although its power consumption is much lower than the PA, the proper adjustment of the noise factor may help the PA to operate in lower consumption modes. Two other important design metrics for the LNA are the voltage gain and the linearity, which control the noise factor and, as a consequence, dictate the sensitivity of the receiver [24]. In the literature, reconfigurable LNA designs usually exploit current or voltage control, impedance variation and feedback control in order to adjust their parameters. For instance, in [25] the proposed LNA has three operating modes and the circuit design is based on a complementary current-reuse common source amplifier, combined with a low-current active feedback. Through reconfiguration, the overall LNA consumption can be reduced by more than 21% in the low-power mode.

Another LNA designed for ultra low power applications targeting the 2.4 GHz band has been proposed by [13], [26]. The circuit design consists of a common gate topology exploiting transistor body biasing while the LNA parameters are reconfigurable via changing the supply voltage. The resulting integrated circuit allows three operating modes, named 'ultra low power mode', 'medium mode' and 'high performance mode'. The voltage gain of each mode is 16.8 dB, 18.8 dB and 21.5 dB, whereas the noise figure is 7.3 dB, 6.7 dB and 6.3 dB, respectively. Besides, the measured power consumption of each mode yields 300 μW, 600 μW and 900 μW, respectively, which is an interesting trade-off between performance and power consumption.

In order to mitigate power consumption at the circuit level, circuit-aware communication designs can be found. For example, the works proposed by [27], [28] illustrate the optimum operating points for the circuit elements of the transceiver as a function of the communication link distance. As a result, they present an optimal bit-resolution for the analog-to-digital converter (ADC), the optimal choice for the noise factor of the LNA and the optimal operating input back-off (IBO) of the PA. In particular, these works do not consider the impact of RF circuits consumption on multiple antenna systems. Furthermore, the approach in [29] tries to search for the most optimized setup at the circuit level, aiming to adapt circuit parameters in real-time in order to reduce the power consumption. However, only the LNA design is addressed in the consumption analysis.

B. CONTRIBUTION

The main contributions of this paper are listed as follows:

- Unlike most works available in the literature, our analysis carefully includes real data from circuits that were previously designed and tested by both simulations and measurements. Our goal is to model the real multimode characteristic of these circuits as look-up tables, which are then handled by our optimization approach. By doing so, any other practical PA or LNA design can be easily integrated into our methodology.
- By exploiting the characteristic of reconfigurable circuits, we achieved more than 75% of energy efficiency improvement for short-range communications in multiple antenna scenarios, compared to the case of non-reconfigurable PA and LNA designs.
- When comparing the MIMO transmission schemes, we show that AS is usually more energy efficient for short and moderate communications, with SVD allowing to communicate at longer distances due to its lower outage probability. It is also observed that the number of antennas contributes differently in AS and SVD schemes. As a result, SVD exhibits an optimal number of antennas in order to maximize the energy efficiency, while the AS energy efficiency monotonically increases with the number of antennas, although a saturation effect is observed with few antennas (four or five) in most scenarios.
- We also demonstrate that there is an optimum spectral efficiency value that maximizes the energy efficiency of each transmission scheme. In addition, we noticed that multiple antenna systems benefit from transmissions with higher spectral efficiency. Further, it has been found that the higher the modulation order, the higher the power back-off and typically a lower output power mode of the PA is required during operation, which contributes towards improving energy efficiency.
- We conclude that the joint reconfiguration of RF amplifiers is fundamental to reduce the energy required to an end-to-end communication, since the LNA allows to improve the SNR by adjusting its gain and, therefore, a lower level of transmit power at the PA output is required.

The remainder of this paper is organized as follows. Section II presents the system model, exposing the characteristics of the reconfigurable PA, LNA, as well as the transmission model. Then, Section III describes the MIMO communication schemes, giving mathematical expressions for the outage probability and energy efficiency of SISO, AS and SVD schemes. Numerical results are given in Section IV and, finally, Section V concludes the paper.

II. SYSTEM MODEL

We consider the transceiver analog signal RF chain depicted by the block diagram in Fig. 1. At the transmitter side, the PA is a reconfigurable RF block, while the other blocks involve the digital-to-analog converter (DAC), mixer, filters and the frequency synthesizer, which have fixed operating points and power consumptions. At the receiver side, the LNA is

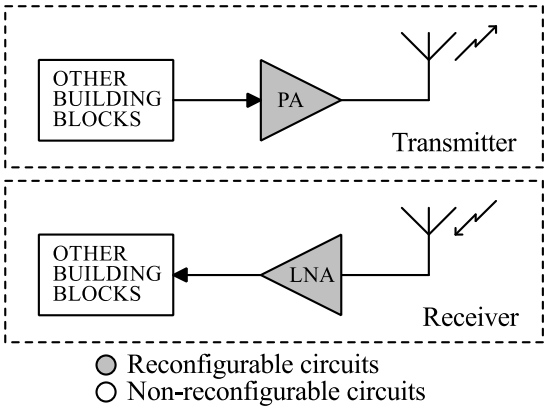

FIGURE 1. RF transceiver building blocks. The circuits in gray are multimode designs.

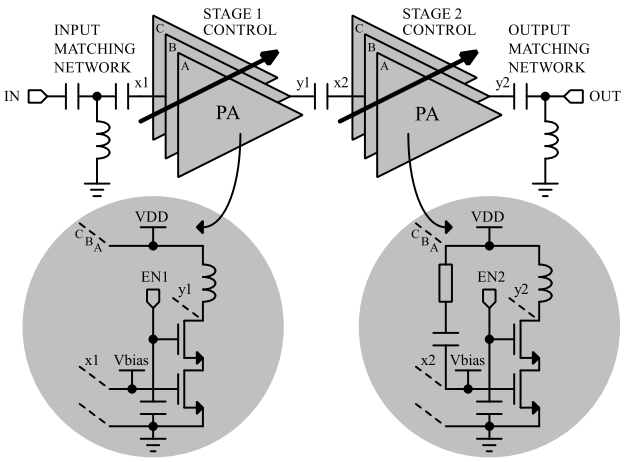

FIGURE 2. Multimode PA circuit design proposed in [12] with gain and power control (bias circuit is omitted).

reconfigurable, while the other blocks with fixed operating points and power consumptions include the mixer, filters, frequency synthesizer, intermediate frequency amplifier (IFA) and the ADC. We denote the number of antennas at the transmitter and at the receiver by n_t and n_r, respectively. In addition, we assume that each RF chain is assembled with a single antenna. Thus, considering that $\hat{n}_t \leq n_t$ RF chains are active at the transmitter and $\hat{n}_r \leq n_r$ RF chains are active at the receiver, the total power consumption can be written as

$$P_{\text{TOTAL}} = \hat{n}_t \left(P_{\text{PA}} + P_{\text{RF,tx}}\right) + \hat{n}_r \left(P_{\text{LNA}} + P_{\text{RF,rx}}\right), \quad (1)$$

where P_{PA} is the power consumed by the PA and P_{LNA} is the power consumed by the LNA, which depend on their respective operating modes, as it will be detailed in Sections II-A and II-B, respectively. In addition, $P_{\text{RF,tx}}$ represents the power consumed by the non-reconfigurable blocks at the transmitter, and $P_{\text{RF,rx}}$ is the equivalent at the receiver.

A. RECONFIGURABLE PA

Typically, the PA has the stronger impact on the total power consumption of the transmitter RF chain, and it depends on the communication distance. The adopted PA follows [12], which is a two-stage class AB PA employing a cascode topology using Globalfoundries 130 nm CMOS technology, operating in the unlicensed 2.4 GHz band.

Fig. 2 illustrates the PA design featuring a power gain stage, an output power stage and two impedance matching networks. The first stage is responsible for the gain control, while the second is a power control stage. In addition, the circuit topology has three cascode cells (A, B and C) at each stage that are controlled by six digital switches (En1A, En1B, En1C, En2A, En2B and En2C). Each switch acts on a cascode cell that is enabled with VDD = 1.8 V and disabled with GND. Therefore, for each activated structure, the width of the effective channel resulting from the transistors increases, and thus the gain and the power increases as well. The combination of these cascode structures provides distinct amplifying characteristics for each cell, yielding 64 possible operating modes. Nevertheless, only 7 out of the 64 operating modes have been selected in this work, those that offer the best performance advantages in terms of power gain, output power and DC power consumption.

Table 1 summarizes the post-layout results for each of the selected operating modes. The operating mode 1 indicates the mode with the lowest power consumption, while mode 7 represents a high-performance mode. As we can observe, the gain (G_{PA}) varies from 18 dB to 31 dB, the saturated output power (P_{TX}) varies from 9.6 dBm to 18.4 dBm, whereas the DC power consumption (P_{PA}) can be as low as 153 mW, up to 394 mW in the high-performance mode.

Conventional linear PAs operate at high efficiency, usually near the peak output power. However, in modulated communication signals these PAs operate at power back-off and, consequently, the efficiency drops off quickly at backed-off power levels. On the other hand, PAs based on multimode operation are more propitious to improve efficiency at power back-off. Table 1 also shows the drain efficiency measured at the 1 dB compression point for the PA under test, denoted as $\eta_{\text{drain@OCP}_{1\text{dB}}}$. For instance, considering a required output power of 15 dBm, mode 5 can be used, yielding a drain efficiency of 11.4% while modes 6 and 7 are still available when higher transmit power is required. Therefore, this PA can be used to enhance efficiency at low output power levels. In addition, the linearity characterization of simplified versions of this PA in the presence of modulated signals for the IEEE 802.11n, IEEE 802.11ax, IEEE 802.15.4 and LTE communication standards can be found in [21] and [30].

It is worthwhile to note that in the case of multiple active RF chains, we assume that the transmit power is uniformilly distributed, so that all PAs operate in the same mode.

B. RECONFIGURABLE LNA

Following the antenna-filter block, the LNA dictates the RF chain sensitivity. The employed LNA in [13] was designed for ultra low power applications and implemented in Fully-Depleted Silicon-On-Insulator (FDSOI) 28 nm ST-Microelectronics technology targeting the 2.4 GHz band.

TABLE 1. Characteristics of the PA for each operating mode at 2.45 GHz.

Operating Mode	Drain Efficiency ($\eta_{\text{drain@OCP}_{1\text{dB}}}$) [%]	Gain (G_{PA}) [dB]	Saturated Output Power (P_{TX}) [dBm]	Power Consumption (P_{PA}) [mW]
1	4.3	18.0	9.6	153
2	8.1	22.2	13.6	214
3	8.9	22.9	14.5	236
4	10.2	26.8	14.7	245
5	11.4	25.0	16.5	297
6	12.6	25.9	17.2	324
7	13.6	31.0	18.4	394

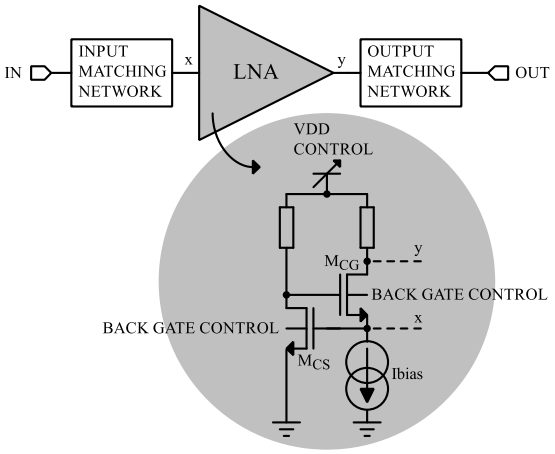

FIGURE 3. Multimode LNA circuit design proposed in [13] with back gate control (bias circuit is omitted).

A simplified schematic of the LNA is reported in Fig. 3. Interestingly input matching is directly achieved by the Common Gate (M_{CG}) stage, and controlled by the bias current (I_{bias}). Unlike conventionnal LNA topologies, the proposed topology does not embed passive devices, such as inductors for input/output matching, dramastically reducing its silicon footprint. This feature reduces the implementation cost of a MIMO system. The amplifier parameters are reconfigurable via supply voltage. However, there is a threshold of VDD = 0.8 V where the parameters are acceptable and there is no other possibility of decreasing the supply voltage while maintaining the design requirements. Therefore, by tuning control through body biasing, the threshold voltage of the transistors is decreased and the power supply voltage can thus be reduced to 0.6 V with a back gate voltage of 2.0 V. This configuration enhances the available gain and enables a reasonable noise factor under low-power constraints.

The noise factor is used to measure the degradation of the SNR, which determines the sensitivity of the receiver. According to the Friis formula [31], the total noise factor at the receiver depends mainly on the first RF block. Hence, the overall noise factor can be expressed as

$$F_{\text{RX,mode}} = F_{\text{LNA,mode}} + \frac{F_{\text{subsequent\_stages}} - 1}{G_{\text{LNA,mode}}}, \tag{2}$$

where $F_{\text{subsequent\_stages}}$ is the noise factor of the subsequent blocks at the receiver RF chain, while $F_{\text{LNA,mode}}$ and $G_{\text{LNA,mode}}$ are the noise factor and the voltage gain of the LNA, respectively, which depend on the operating mode. Table 2 summarizes the LNA measured performance for its three operating modes. As we can observe, since the LNA gain is high ($G_{\text{LNA}} \geq 16.8$ dB), the noise factor of the receiver can be well approximated by the noise factor of the LNA, *i.e.*, $F_{\text{RX,mode}} \approx F_{\text{LNA,mode}}$.

Furthermore, the power consumption of the LNA (P_{LNA}) is also obtained from Table 2, with $P_{\text{LNA}} \in \{0.3, 0.6, 0.9\}$ mW for each respective operating mode. In addition, the LNA linearity was evaluated by measuring the third order input intercept point (IIP3), been constant at -16 dBm for the three operating modes.

C. COMMUNICATION MODEL

A transmission connecting two nodes can be represented in the following vector form:

$$\mathbf{y} = \sqrt{\kappa\, P_{\text{TX,mode}}}\, \mathbf{H}\, \mathbf{x} + \mathbf{w}, \tag{3}$$

where $\mathbf{y} \in \mathbb{C}^{\hat{n}_{\text{r}} \times 1}$ is the received vector, $P_{\text{TX,mode}}$ is the transmit power depending on the operating mode of the PA, κ is the link budget relationship, $\mathbf{H} \in \mathbb{C}^{\hat{n}_{\text{r}} \times \hat{n}_{\text{t}}}$ is the matrix of quasi-static channel coefficients, whose elements $h_{ij} \in \mathbf{H}$, $\forall i, j$, are independent and identically distributed (i.i.d.) random variables with zero-mean and unit-variance Rayleigh distribution. Furthermore, $\mathbf{x} \in \mathbb{C}^{\hat{n}_{\text{t}} \times 1}$ is the unit energy transmitted symbol vector and $\mathbf{w} \in \mathbb{C}^{\hat{n}_{\text{r}} \times 1}$ is the additive white Gaussian noise (AWGN) vector, with variance $N_0/2$ per dimension, where N_0 is the unilateral thermal noise power spectral density. The link budget relationship is assumed to be given by [6]

$$\kappa = \frac{G_{\text{A}}\, \lambda^2}{(4\pi)^2\, d^{\alpha}\, M_{\text{L}}\, F_{\text{RX,mode}}}, \tag{4}$$

where G_{A} is the total antenna gains, $\lambda = \frac{3.10^8}{f_{\text{c}}}$ is the wavelength, f_{c} is the carrier frequency, d is the distance between communicating nodes, α is the path loss exponent, and M_{L} is the link margin. In addition, the instantaneous SNR at the receiver is

$$\gamma = \|\mathbf{H}\|_F^2 \cdot \bar{\gamma}, \tag{5}$$

where $\|.\|_F$ is the Frobenius norm and $\bar{\gamma} = \frac{P_{\text{TX,mode}} \cdot \kappa}{N_0 \cdot B}$ is the average SNR per active transmit antenna.

Notice that the operating modes of the PA and the LNA impact the average SNR at the receiver. Therefore, the joint adaptation of these modes impacts the energy efficiency.

[1] Let us remark that the noise factor (F) is linear and the noise figure (NF) is expressed in decibels (dB).

TABLE 2. Characteristics of the LNA for each operating mode at 2.4 GHz.

Operating Mode	Linearity (IIP3_{LNA}) [dBm]	Gain (G_{LNA}) [dB]	Noise Figure[1] (NF_{LNA}) [dB]	Power Consumption (P_{LNA}) [mW]
1	−16	16.8	7.3	0.3
2	−16	18.8	6.7	0.6
3	−16	21.5	6.3	0.9

III. TRANSMISSION SCHEMES

In this section we present two MIMO transmission schemes: *(i)* antenna selection (AS), in which a single pair of antennas is activated at the transmitter and receiver, requiring a single RF chain at each side; and *(ii)* MIMO beamforming scheme based on singular value decomposition (SVD), which uses all transmit and receive antennas in order to improve reliability. In addition, the SISO scheme is also considered for comparison. Finally, we consider as performance metrics the outage probability and the energy efficiency.

A. SISO

In the SISO scheme, there is a single antenna at each transmit/receive node ($n_{\text{t}} = n_{\text{r}} = 1$), so that we can denote the single channel coefficient by h. Then, the mutual information between TX and RX is given by [6]

$$I_{\text{SISO}} = B\,\log_2\left(1+\bar{\gamma}\cdot h^2\right), \tag{6}$$

so that an outage event occurs whenever I_{SISO} falls below the bit rate $R_{\text{b}} = \xi\cdot B$, where ξ is the spectral efficiency in bps/Hz. Thus, assuming Rayleigh fading, the outage probability of the SISO transmission is given by [6]

$$\mathcal{O}_{\text{SISO}} = \Pr\{I_{\text{SISO}} < R_{\text{b}}\} = 1-\exp\left(-\frac{2^{\xi}-1}{\bar{\gamma}}\right). \tag{7}$$

Furthermore, we also express the energy efficiency of the SISO scheme in terms of bits/J/Hz as

$$\eta_{\text{SISO}} = \frac{\xi\cdot(1-\mathcal{O}_{\text{SISO}})}{P_{\text{PA}}+P_{\text{RF,tx}}+P_{\text{LNA}}+P_{\text{RF,rx}}}, \tag{8}$$

where the numerator represents the system throughput, in bps/Hz, while the denominator is the total power consumption of the SISO scheme.

B. ANTENNA SELECTION (AS)

In the case of AS, a single RF chain ($\hat{n}_{\text{t}} = 1$) out of n_{t} is selected at the transmitter, while $\hat{n}_{\text{r}} = 1$ out of n_{r} antennas is selected at the receiver. Since the pair of antennas is activated in order to maximize the instantaneous SNR, the mutual information of the AS scheme can be written as

$$I_{\text{AS}} = B\,\log_2\left(1+\bar{\gamma}\cdot\max_{i,j} h_{ij}^2\right), \tag{9}$$

so that the outage probability of AS follows [9]

$$\mathcal{O}_{\text{AS}} = \left[1-\exp\left(-\frac{2^{\xi}-1}{\bar{\gamma}}\right)\right]^{n_{\text{t}}n_{\text{r}}}. \tag{10}$$

Finally, the energy efficiency of AS is

$$\eta_{\text{AS}} = \frac{\xi\cdot(1-\mathcal{O}_{\text{AS}})}{P_{\text{PA}}+P_{\text{RF,tx}}+P_{\text{LNA}}+P_{\text{RF,rx}}}, \tag{11}$$

where, we remark that although (11) is very similar to (8), the outage probability of AS is lower than that of SISO, due to the exponent $n_{\text{t}}n_{\text{r}}$ in (10), while the power consumption is similar, once a single RF chain is active at each side in both schemes. Thus, it is expected that AS yields a higher energy efficiency than SISO.

C. SINGULAR VALUE DECOMPOSITION (SVD) BEAMFORMING

The use of beamforming through the SVD technique allows to exploit all $\hat{n}_{\text{t}} = n_{\text{t}}$ and $\hat{n}_{\text{r}} = n_{\text{r}}$ antennas at once. The mutual information of the SVD scheme is given by [32]

$$I_{\text{SVD}} = B\,\log_2\left[\det\left(\mathbf{I}_n+\bar{\gamma}\cdot\mathbf{H}\mathbf{H}^{\dagger}\right)\right], \tag{12}$$

$$= B\sum_{l=1}^{n}\log_2\left(1+\bar{\gamma}\cdot\lambda_l^2\right), \tag{13}$$

where $\mathbf{I}_n$ is an identity matrix, $n = \min\{n_{\text{t}}, n_{\text{r}}\}$, † denotes the conjugate transpose operation, and λ_l are the eigenvalues of $\mathbf{H}\mathbf{H}^{\dagger}$. In addition, the transformation from (12) to (13) follows the SVD operation [32]. Using Jensen's inequality, the mutual information of SVD can be upper bounded by [32]

$$\frac{1}{n}\sum_{l=1}^{n}\log_2\left(1+\bar{\gamma}\cdot\lambda_l^2\right) \le \log_2\left(1+\frac{\bar{\gamma}}{n}\sum_{l=1}^{n}\lambda_l^2\right), \tag{14}$$

and since $\sum_{l=1}^{n}\lambda_l^2 = \sum_{i,j}h_{ij}^2$, then the outage probability of SVD becomes [9]

$$\mathcal{O}_{\text{SVD}} \ge 1-\exp\left(-\frac{\rho}{\bar{\gamma}}\right)\sum_{m=0}^{n_{\text{t}}n_{\text{r}}-1}\frac{1}{m!}\cdot\left(\frac{\rho}{\bar{\gamma}}\right)^{m}, \tag{15}$$

where $\rho = n\cdot\left(2^{\xi/n}-1\right)$. Then, the energy efficiency of SVD can be expressed by

$$\eta_{\text{SVD}} \le \frac{\xi\cdot(1-\mathcal{O}_{\text{SVD}})}{n_{\text{t}}\left(P_{\text{PA}}+P_{\text{RF,tx}}\right)+n_{\text{r}}\left(P_{\text{LNA}}+P_{\text{RF,rx}}\right)}. \tag{16}$$

Since the mutual information of SVD is higher than that of AS and SISO [32], it yields the highest throughput compared to the other schemes. On the other hand, since all RF chains are active, the power consumption is also higher, which may present a few trade-offs in terms of energy efficiency compared to SISO and AS. In addition, let us remark that the energy efficiency in (16) is an optimistic result, since the outage probability of SVD is lower bounded in our analysis.

D. OPTIMIZATION PROBLEM

In order to maximize the energy efficiency of the communication system, we aim at a joint selection of the best operating modes for the PA and the LNA circuits. The operating mode of the PA dictates the employed transmit power, while the operating mode of the LNA modifies the sensitivity of the receiver. Besides, we also assume that the spectral efficiency can be proper adjusted by changing modulation and coding at the transmitter. Thus, our optimization problem becomes

$$\max_{P_{\mathrm{TX,mode}},F_{\mathrm{RX,mode}},\xi} \quad \eta_{\mathrm{sch}}, \tag{17a}$$

$$\text{s.t.} \quad P_{\mathrm{TX,mode}} \in \mathcal{S}_{\mathrm{PA}}, \tag{17b}$$

$$F_{\mathrm{RX,mode}} \in \mathcal{S}_{\mathrm{LNA}}, \tag{17c}$$

$$\xi \geq 0, \tag{17d}$$

$$\mathcal{O}_{\mathrm{sch}} \leq \mathcal{O}^{\star}, \tag{17e}$$

where the subscript sch $\in$ {SISO, AS, SVD} represents each of the considered transmit schemes, $\mathcal{S}_{\mathrm{PA}}$ is the set of transmit powers provided by the 7 operating modes of the PA, according to Table 1, $\mathcal{S}_{\mathrm{LNA}}$ is the set of the noise factors yielded by the 3 operating modes of the LNA, according to Table 2, and $\mathcal{O}^{\star}$ represents a target outage probability at the receiver.

In addition, due to the optimization of the spectral efficiency, the power back-off effect of the PA must be considered for higher modulations orders. In order to model the power loss due to the back-off, we assume the use of an M-QAM modulation, with spectral efficiency $\xi = \log_2(M)$, where M is the modulation order, so that the PAPR is [33]

$$\mathrm{PAPR}(\xi) = 3 \cdot \frac{\sqrt{2^{\xi}} - 1}{\sqrt{2^{\xi}} + 1}, \tag{18}$$

and the effective transmit power of the PA, in dBm, is

$$\tilde{P}_{\mathrm{TX,mode}} = P_{\mathrm{TX,mode}} - \mathrm{PAPR}(\xi). \tag{19}$$

Algorithm 1 details the employed approach in order to jointly optimize $P_{\mathrm{TX,mode}}$, $F_{\mathrm{RX,mode}}$ and ξ. Due to the limited solution space, we resort to an exhaustive search to solve the optimization problem in (17a), in which $\mathcal{S}_{\xi}$ is the set of available spectral efficiencies. Notice that this set depends on the particular employed RF transceiver, as it is a functon of the available choices for modulation and code rates. Furthermore, the variables $P_{\mathrm{TX,mode}}$ and $F_{\mathrm{RX,mode}}$ also belong to discrete sets. Therefore, a look-up table (LUT) can be easily implemented in practice, with the size of the LUT being $|\mathcal{S}_{\xi}| \times |\mathcal{S}_{\mathrm{PA}}| \times |\mathcal{S}_{\mathrm{LNA}}|$, where $|.|$ represents the cardinality of the set. Therefore, $21 \times |\mathcal{S}_{\xi}|$ entries for the LUT are required in our problem, in which we consider a large set for $\mathcal{S}_{\xi}$ in our simulations. However, $|\mathcal{S}_{\xi}|$ may be quite small in practice, so that the complexity of the proposed solution is small.

Furthermore, we also assume that the adaptation of the PA and LNA operating modes is done during the transmission of pilot symbols prior to each frame. Let us remark that the pilot symbols exchange is already required for channel estimation due to the MIMO transmission schemes. As a consequence, only a few aditional bits are required, depending on the number of available modes.

Algorithm 1 Maximization of the Energy Efficiency for Each Transmission Scheme sch $\in$ {SISO, AS, SVD}

Input: d, $\mathcal{O}^{\star}$

$i \leftarrow 1$; $\eta_{\mathrm{sch},i-1} \leftarrow 0$
for $\xi \in \mathcal{S}_{\xi}$ **do**
  for $P_{\mathrm{TX,mode}} \in \mathcal{S}_{\mathrm{PA}}$ **do**
    ; compute $\tilde{P}_{\mathrm{TX,mode}} = P_{\mathrm{TX,mode}} - \mathrm{PAPR}(\xi)$
    for $F_{\mathrm{RX,mode}} \in \mathcal{S}_{\mathrm{LNA}}$ **do**
      ; compute $P_{\mathrm{PA,mode}}$ and $P_{\mathrm{LNA,mode}}$
      ; compute κ and $\bar{\gamma}$ using (4)
      if $\mathcal{O}_{\mathrm{sch}} > \mathcal{O}^{\star}$ **then**
        $\eta_{\mathrm{sch},i} \leftarrow 0$
      else
        ; compute $\eta_{\mathrm{sch},i}$ using (8), (11) or (16)
        if $\eta_{\mathrm{sch},i} < \eta_{\mathrm{sch},i-1}$ **then**
          $\eta_{\mathrm{sch},i} \leftarrow \eta_{\mathrm{sch},i-1}$
        end if
      end if
    end for
  end for
end for

Output: $\eta_{\mathrm{sch},i}$

TABLE 3. System parameters used for the numerical examples.

Parameter	Description	Value
B	bandwidth	10 kHz
M_{L}	link margin	30 dB
f_{c}	carrier frequency	2.4 GHz
G_{A}	total antenna gain	5 dBi
α	path loss exponent	2.5
$\mathcal{O}^{\star}$	target outage probability	10^{-3}
N_0	noise power spectral density	-174 dBm/Hz
$P_{\mathrm{RF,tx}}$	non-reconf. TX power consumption	97.9 mW
$P_{\mathrm{RF,rx}}$	non-reconf. RX power consumption	92.2 mW

IV. NUMERICAL RESULTS

In this section we present a few numerical examples considering our proposed optimization approach. The simulation parameters are defined in Table 3, following [34]. Furthermore, we compare the performance of the reconfigurable PA and LNA described in Sections II-A and II-B, respectively, with two state-of-the-art non-reconfigurable designs from the literature. The chosen PA and LNA used for comparison aim at high-performance only. In other words, their design focus on good performance in terms of high output power for the PA and low noise factor for the LNA, rather than having reconfigurable capabilities. We employ the PA proposed by [14], which consumes $P_{\mathrm{DC}} = 392.5$ mW at 2.4 GHz, yielding a saturated output power of $P_{\mathrm{TX}} = 24$ dBm, with a peak drain efficiency of 64%. In addition, the LNA proposed by [15] consumes $P_{\mathrm{DC}} = 1.32$ mW, providing a noise figure of 4 dB at 2.4 GHz.

A. ENERGY EFFICIENCY WITH RECONFIGURABLE RF CIRCUITS AND FIXED SPECTRAL EFFICIENCY

First, let us consider the case when the optimization problem in (17a) is solved for a fixed spectral efficiency, *i.e.*, only the

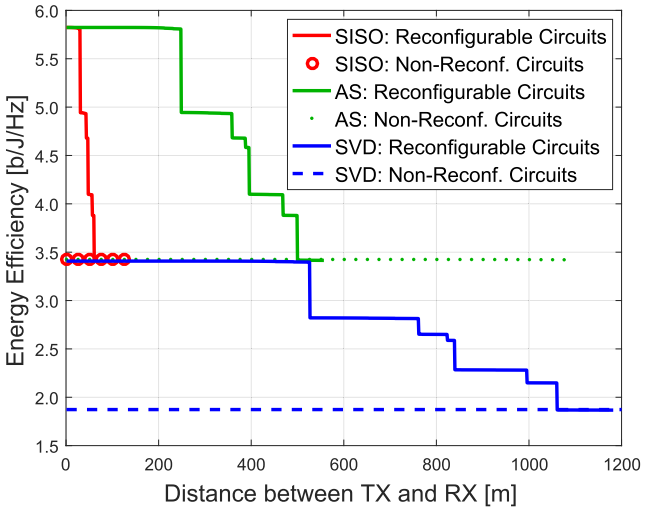

FIGURE 4. Energy efficiency of SISO, AS and SVD, comparing reconfigurable and non-reconfigurable circuits, when $\xi = 2$ bps/Hz and $n_t = n_r = 2$ antennas.

effect of the PA and LNA operating modes are considered. Fig. 4 plots the energy efficiency of SISO, AS and SVD as a function of the communication distance when $n_t = n_r = 2$ antennas and $\xi = 2$ bps/Hz, which corresponds to a PAPR = 0 dB. A first important observation can be drawn comparing the transmission schemes. Notice that the curves appear to be incomplete, since each scheme can only transmit up to a given range due to the QoS constraint ($\mathcal{O}_{sch} \leq \mathcal{O}^{\star}$). Therefore, we observe that AS outperforms the other schemes in terms of energy efficiency, but SVD allows longer communication distances, which may be important to some MTC applications. In addition, a second important observation from Fig. 4 is the comparison between reconfigurable and non-reconfigurable designs. For short-range communications, the energy efficiency obtained using the reconfigurable circuits is significantly higher compared to the non-reconfigurable circuits. As we can see, at distances up to 200 meters, an energy gain above 81% for SVD and 75% for AS is achieved, while for SISO we observe an improvement in distances of up to 50 meters. As a conclusion, to significantly reduce the energy required an end-to-end communication, the proposed approach shows that the design and development of reconfigurable RF circuits is crucial towards improving energy efficiency of modern applications, which have very distinct communication ranges. Besides, we also observe that the performance using non-reconfigurable circuits becomes better at longer distances. Such behavior occurs since the circuits from [14], [15], as most of the approaches for the constructions of PAs and LNAs, are designed for these operating points. Thus, these circuits can be optimized for long distances, sacrificing reconfigurability. For instance, the PA from [14] provides a transmit power of $P_{TX} = 24$ dBm, while the mode 7 of the PA from Section II-A yields $P_{TX} = 18.4$ dBm. More significantly, the noise figure of the LNA from [15] is 4 dB, while the noise figure of the mode 3 of the LNA from Section II-B is 6.3 dB.

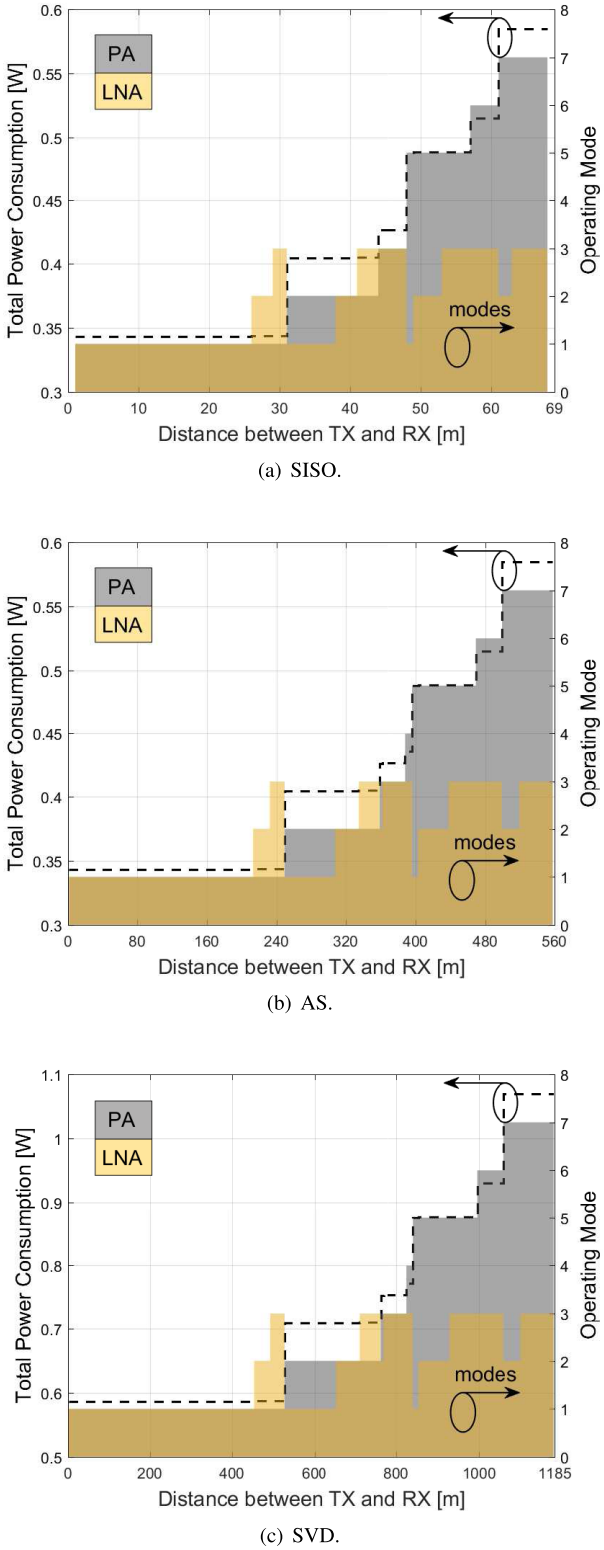

(a) SISO.

(b) AS.

(c) SVD.

FIGURE 5. Overall power consumption and best operating mode for the PA and the LNA, of SISO, AS and SVD schemes, when $\xi = 2$ bps/Hz and $n_t = n_r = 2$ antennas.

Fig. 5 complements the analysis, showing the total power consumption of SISO, AS and SVD schemes, represented by the black dashed lines and the axis on the left side of the figure. In addition, the operating mode of the PA and LNA

circuits are also shown as a function of the communication distance, represented by the colored bars and the axis on the right side of the figure. A first observation shows that the reconfigurable LNA has greater influence over short communication distances, as expected since its consumption is lower when compared to the PA. Besides, the PA remains in the lowest-power consumption point (mode 1) as much as possible, while the LNA switches its operating mode with the increase of the distance in order to improve the sensitivity at the receiver. When it is not possible to improve the sensitivity even further by changing the LNA operating mode, then the PA operating mode changes to increase the transmit power. After the PA switches its operating mode, we observe that the LNA returns to a lower operating mode in order to adjust the RF signal gain at the receiver. Furthermore, we can also conclude that the power consumption of AS is similar to that of SISO, whereas SVD consumes considerably more power at the circuit level.

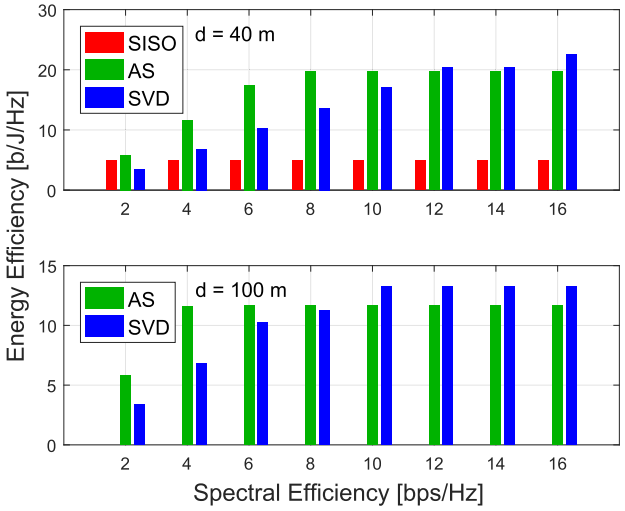

FIGURE 6. Energy efficiency versus spectral efficiency with reconfigurable circuits, when $n_t = n_r = 2$ antennas.

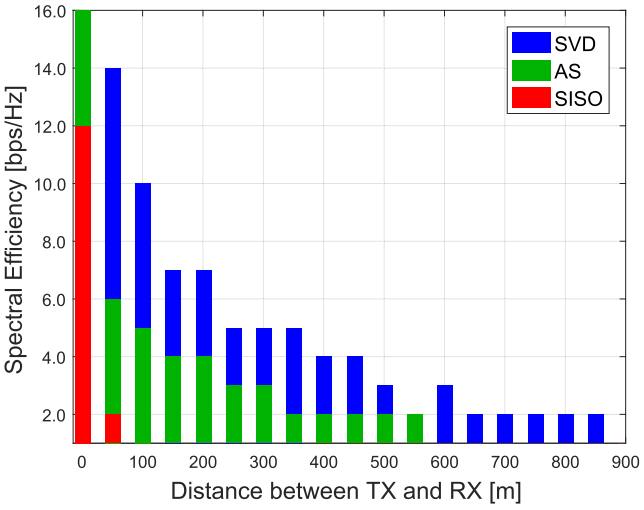

FIGURE 7. Optimum spectral efficiency as a function of the communication distance, when $n_t = n_r = 2$ antennas.

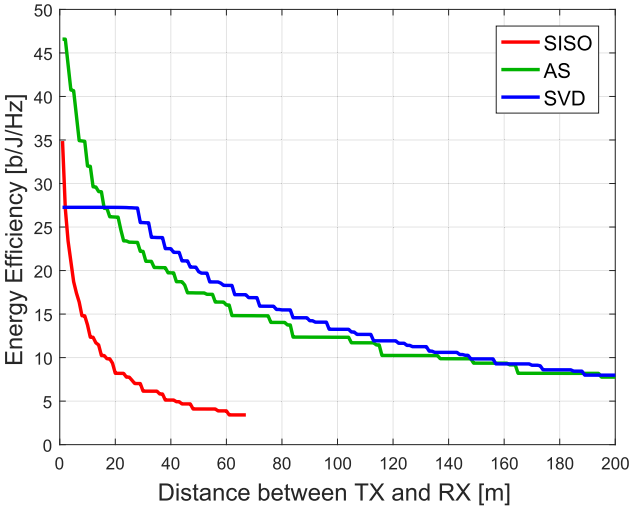

FIGURE 8. Energy efficiency of SISO, AS and SVD schemes jointly optimizing the PA and LNA operating modes, as well as the spectral efficiency, when $n_t = n_r = 2$ antennas.

B. ENERGY EFFICIENCY WITH RECONFIGURABLE RF CIRCUITS AND OPTIMIZED SPECTRAL EFFICIENCY

In this subsection, we optimize the spectral efficiency along with the PA and LNA operating modes, in order to solve (17a). First, Fig. 6 depicts the energy efficiency as a function of the spectral efficiency for two link distances between transmitter and receiver. From the figure we observe that the spectral efficiency contributes to maximize the energy efficiency. Interestingly, there is an optimum spectral efficiency value that maximizes each transmission scheme. The optimal ξ for each scheme is shown in Fig. 7 as a function of the transmit distance. As we observe, the RF signal is transmitted with high spectral efficiency for short-range communications, since the communication channel has higher SNR. However, when the distance increases the spectral efficiency decreases to meet the target outage probability at the receiver.

Fig. 8 illustrates the energy efficiency of SISO and MIMO schemes. First, comparing with Fig. 4 we observe a significant gain in terms of energy efficiency, followed by an increase in the communication link distance for all schemes under analysis. We can also note an 'oscillation' in the energy efficiency curve that reflects the switching of the PA and LNA operating modes along with the spectral efficiency optimization. Further, it is important to note that SISO and AS are more energy-efficient than SVD for very short distances. Nevertheless, very high spectral efficiencies are used by the SVD scheme in this analysis, which in practice will be limited by the available modes for modulation and coding at the transceiver.

Fig. 9 depicts the selected operating modes for the PA and LNA circuits as a function of the communication distance, as well as the total power consumption. Compared to Fig. 5, where the total power consumption is a non-decreasing function of the transmit distance, here the total power consumption oscillates a bit more since the PA changes its operating

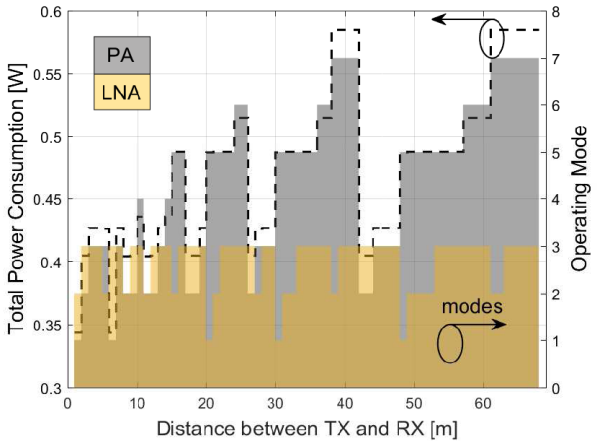

(a) SISO.

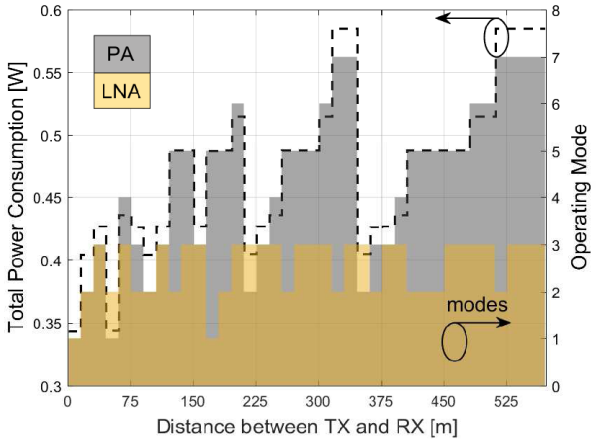

(b) AS.

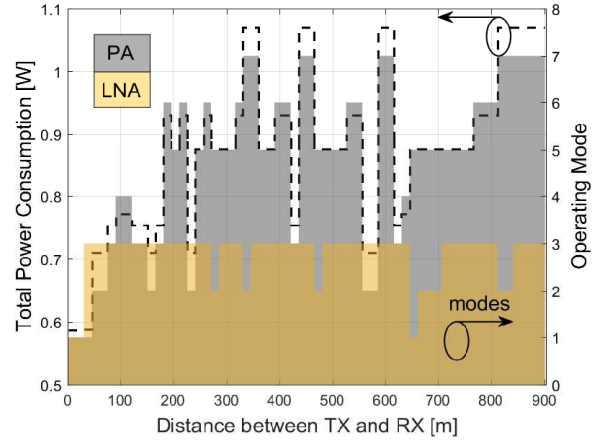

(c) SVD.

FIGURE 9. Overall power consumption and best operating mode for the PA and LNA, of SISO, AS and SVD schemes, when optimizing the spectral efficiency with $n_t = n_r = 2$ antennas.

modes more constantly. Such interesting behavior can be explained by the reconfiguration of spectral efficiency in order to maintain an acceptable communication quality given by the target outage. Therefore, depending on the spectral

TABLE 4. PA parameters for each transmission scheme, considering different spectral efficiency values as a function of the transmit distance, indicating the PA operating mode, PAPR, output power and drain efficiency at power back-off.

SISO					
d [m]	PA mode	ξ [bps/Hz]	PAPR(ξ) [dB]	$\tilde{P}_{\mathrm{TX,mode}}$ [dBm]	$\eta_{\mathrm{drain@BO}}$ [%]
10	2	5	3.2	10.4	5.1
20	5	4	2.6	14	8.4
30	5	3	1.6	15	10.6
40	7	3	1.6	16.9	12.3
50	5	2	0	16.5	15.2
AS					
d [m]	PA mode	ξ [bps/Hz]	PAPR(ξ) [dB]	$\tilde{P}_{\mathrm{TX,mode}}$ [dBm]	$\eta_{\mathrm{drain@BO}}$ [%]
10	1	11	4.6	5	2.1
20	1	9	4.4	5.2	2.2
30	3	9	4.4	10.1	4.3
40	2	8	4.2	9.4	4.1
50	1	6	3.7	5.9	2.6
SVD					
d [m]	PA mode	ξ [bps/Hz]	PAPR(ξ) [dB]	$\tilde{P}_{\mathrm{TX,mode}}$ [dBm]	$\eta_{\mathrm{drain@BO}}$ [%]
10	1	16	4.7	4.9	2
20	1	16	4.7	4.9	2
30	1	15	4.7	4.9	2
40	1	13	4.7	4.9	2
50	2	14	4.7	8.9	3.6

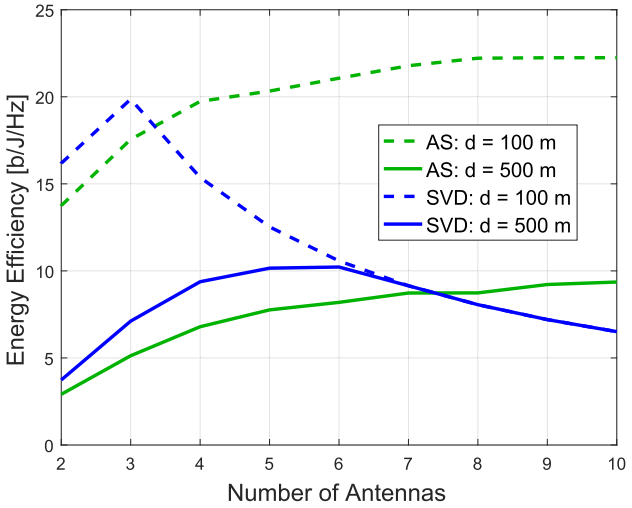

FIGURE 10. Energy efficiency versus the number of antennas with $n_t = n_r$.

efficiency, the reconfigurable amplifiers adapt their operating modes in order to enhance the energy efficiency.

Table 4 complements the analysis. First, we note that the lower the communication distance, the higher the modulation order with a lower PA operating mode. According to Figures 7 and 9, as the distance increases, the modulation order decreases and the PA used higher operating modes. Further, it is worth noting that the PAPR is limited to 4.8 dB, which is obtained when M tends to infinity. As a consequence, the PAPR effect forces the PA to back-off the maximum average transmit power and, therefore, decreases the PA efficiency. For example, with a spectral efficiency of 16 bps/Hz, which reflects in PAPR $=$ 4.7 dB, and considering the PA in mode 1, we can see that the average output

power drops to 4.9 dBm with a drain efficiency measured at power back-off of $\eta_{\text{drain@BO}} = 2\%$, which is lower than the drain efficiency measured at the 1 dB compression point of $\eta_{\text{drain@OCP}_{\text{1dB}}} = 4.3\%$ as in Table 1.

Finally, Fig. 10 evaluates the energy efficiency as a function of the number of antennas, which we consider to be the same in both transmitter and receiver. Considering the communication distances under analysis 100 m and 500 m, we note that when we increase the number of antennas, AS achieves higher energy efficiency, but this increase in performance saturates after a certain number of antennas. In the case of SVD, there is an optimum number of antennas with the reconfigurable approach that optimizes the energy efficiency. In our examples, 3×3 antennas is optimal for $d = 100$ m, while a 6×6 arrangement is optimal for $d = 500$ m.

V. CONCLUSION

Modern MTC networks have an increasing concern towards higher energy efficiency, since MTC nodes are usually battery-powered. In this paper, we have analyzed the energy efficiency of reconfigurable circuit designs, showing that RF transceivers based on multimode operation can significantly improve the energy efficiency in MIMO communication scenarios. In our framework, we have considered state-of-the-art reconfigurable PA and LNA designs, which are the blocks responsible for RF amplification and, thus, are typically power-hungry. Our results have shown that by reconfiguring the PA operating modes at the transmitter jointly with the LNA operating modes at the receiver, more than 75% of energy efficiency is achieved for short-range communications when compared to non-reconfigurable circuit designs. Further, we also considered that the PA operates at different backed-off power levels under different spectral efficiency values. Generally, increasing the modulation order provides spectral efficiency advantage, but this leads to an increase in PAPR at the price of energy efficiency. However, we showed that combining spectral efficiency with reconfigurable circuits, an even more significant gain in energy efficiency can be achieved for the same scenario under test. In addition, our results also pointed out that AS is in general more energy efficient than the other schemes in several communication scenarios, whereas SVD achieves longer distances of communication. Finally, we also conclude that the number of antennas for MIMO schemes contribute differently to energy efficiency. SVD presents an optimal number of antennas, since the energy efficiency decreases due to the increase of RF chains. On the other hand, the energy efficiency of the AS always increases with the number of antennas, although the increase saturates at a certain point.

REFERENCES

[1] H. Shariatmadari, R. Ratasuk, S. Iraji, A. Laya, T. Taleb, R. Jäntti, and A. Ghosh, "Machine-type communications: Current status and future perspectives toward 5G systems," *IEEE Commun. Mag.*, vol. 53, no. 9, pp. 10–17, Sep. 2015.

[2] A. Holfeld, D. Wieruch, L. Raschkowski, T. Wirth, C. Pallasch, W. Herfs, and C. Brecher, "Radio channel characterization at 5.85 GHz for wireless M2M communication of industrial robots," in *Proc. IEEE Wireless Commun. Netw. Conf. (WCNC)*, Apr. 2016, pp. 1–7.

[3] G. A. Akpakwu, B. J. Silva, G. P. Hancke, and A. M. Abu-Mahfouz, "A survey on 5G networks for the Internet of Things: Communication technologies and challenges," *IEEE Access*, vol. 6, pp. 3619–3647, 2018.

[4] *The Internet of Things Business Index 2017: Transformation in Motion*, Economist Intell. Unit, London, U.K., 2017.

[5] M. R. Palattella, M. Dohler, A. Grieco, G. Rizzo, J. Torsner, T. Engel, and L. Ladid, "Internet of Things in the 5G era: Enablers, architecture, and business models," *IEEE J. Sel. Areas Commun.*, vol. 34, no. 3, pp. 510–527, Mar. 2016.

[6] A. Goldsmith, *Wireless Communications*, 1st ed. Cambridge, U.K.: Cambridge Univ. Press, 2005.

[7] *2.4 GHz to 2.5 GHz 802.11g/b RF Transceiver, PA, Rx/Tx/Antenna Diversity Switch*, Maxim Integr., San Jose, CA, USA, 2011.

[8] "CC13xx antenna diversity," Texas Instrum., Dallas, TX, USA, Appl. Rep. SWRA523B, Sep. 2016.

[9] G. Brante, I. Stupia, R. D. Souza, and L. Vandendorpe, "Outage probability and energy efficiency of cooperative MIMO with antenna selection," *IEEE Trans. Wireless Commun.*, vol. 12, no. 11, pp. 5896–5907, Nov. 2013.

[10] E. L. Santos, B. Leite, and A. Mariano, "Multimode 2.4 GHz CMOS power amplifier with gain control for efficiency enhancement at power backoff," in *Proc. IEEE 6th Latin Amer. Symp. Circuits Syst. (LASCAS)*, Feb. 2015, pp. 1–4.

[11] J.-M. Hannula, M. Kosunen, A. Lehtovuori, K. Rasilainen, K. Stadius, J. Ryynänen, and V. Viikari, "Performance analysis of frequency-reconfigurable antenna cluster with integrated radio transceivers," *IEEE Antennas Wireless Propag. Lett.*, vol. 17, no. 5, pp. 756–759, May 2018.

[12] B. Y. Tarui, F. Santos, E. L. Santos, B. Leite, and A. Mariano, "Design of an RF six-mode CMOS power amplifier for efficiency improvement at power backoff," in *Proc. 31st Symp. Integr. Circuits Syst. Design (SBCCI)*, Aug. 2018, pp. 1–6.

[13] J. Zaini, F. Hameau, T. Taris, D. Morche, P. Audebert, and E. Mercier, "A tunable ultra low power inductorless low noise amplifier exploiting body biasing of 28 nm FDSOI technology," in *Proc. IEEE/ACM Int. Symp. Low Power Electron. Design (ISLPED)*, Jul. 2017, pp. 1–6.

[14] M. Thian, V. Fusco, and P. Gardner, "Power-combining class-E amplifier with finite choke," *IEEE Trans. Circuits Syst. I, Reg. Papers*, vol. 58, no. 3, pp. 451–457, Mar. 2011.

[15] F. Belmas, F. Hameau, and J. Fournier, "A low power inductorless LNA with double *G_m* enhancement in 130 nm CMOS," *IEEE J. Solid-State Circuits*, vol. 47, no. 5, pp. 1094–1103, May 2012.

[16] H. S. Ruiz and R. B. Pérez, "Impact of PA on integrated transceivers," in *Linear CMOS RF Power Amplifiers: A Complete Design Workflow*, 1st ed. Springer, 2014.

[17] Y. Yoon, J. Kim, H. Kim, K. H. An, O. Lee, C. Lee, and J. S. Kenney, "A dual-mode CMOS RF power amplifier with integrated tunable matching network," *IEEE Trans. Microw. Theory Techn.*, vol. 60, no. 1, pp. 77–88, Jan. 2012.

[18] K. H. An, D. H. Lee, O. Lee, H. Kim, J. Han, W. Kim, C. Lee, H. Kim, and J. Laskar, "A 2.4 GHz fully integrated linear CMOS power amplifier with discrete power control," *IEEE Microw. Wireless Compon. Lett.*, vol. 19, no. 7, pp. 479–481, Jul. 2009.

[19] S. A. Z. Murad, R. K. Pokharel, H. Kanaya, and K. Yoshida, "A 2.4 GHz 0.18-μm CMOS class E single-ended power amplifier without spiral inductors," in *Proc. Top. Meeting Silicon Monolithic Integr. Circuits RF Syst. (SiRF)*, Jan. 2010, pp. 25–28.

[20] J. Kim, Y. Yoon, H. Kim, K. H. An, W. Kim, H. Kim, C. Lee, and K. T. Kornegay, "A linear multi-mode CMOS power amplifier with discrete resizing and concurrent power combining structure," *IEEE J. Solid-State Circuits*, vol. 46, no. 5, pp. 1034–1048, May 2011.

[21] E. L. Santos, M. A. Rios, L. Schuartz, B. Leite, L. Lolis, E. G. Lima, and A. A. Mariano, "A fully integrated CMOS power amplifier with discrete gain control for efficiency enhancement," *Microelectron. J.*, vol. 70, pp. 34–42, Dec. 2017.

[22] K. Mimis, S. Wang, and G. T. Watkins, "A load-modulated low-power amplifier with average power tracking," in *Proc. Eur. Microw. Conf. (EuMC)*, Sep. 2015, pp. 88–91.

[23] T. Das, "Practical considerations for low noise amplifier design," NXP, Eindhoven, The Netherlands, White Paper, 2013.

[24] S. Mateos-Angulo, D. Mayor-Duarte, S. L. Khemchandani, and J. del Pino, "A low-power fully integrated CMOS RF receiver for 2.4-GHz-band IEEE 802.15.4 standard," in *Proc. Conf. Design Circuits Integr. Syst. (DCIS)*, Nov. 2015, pp. 1–6.
[25] M. De Souza, A. Mariano, and T. Taris, "Reconfigurable inductorless wideband CMOS LNA for wireless communications," *IEEE Trans. Circuits Syst. I, Reg. Papers*, vol. 64, no. 3, pp. 675–685, Mar. 2017.
[26] J. Zaini-Desevedavy, F. Hameau, T. Taris, D. Morche, and P. Audebert, "An ultra-low power 28 nm FD-SOI low noise amplifier based on channel aware receiver system analysis," *J. Low Power Electron. Appl.*, vol. 8, no. 2, p. 10, 2018.
[27] A. Mezghani, N. Damak, and J. A. Nossek, "Circuit aware design of power-efficient short range communication systems," in *Proc. 7th Int. Symp. Wireless Commun. Syst.*, Sep. 2010, pp. 869–873.
[28] A. Mezghani and J. A. Nossek, "Power efficiency in communication systems from a circuit perspective," in *Proc. IEEE Int. Symp. Circuits Syst. (ISCAS)*, May 2011, pp. 1896–1899.
[29] D. Banerjee, B. Muldrey, X. Wang, S. Sen, and A. Chatterjee, "Self-learning RF receiver systems: Process aware real-time adaptation to channel conditions for low power operation," *IEEE Trans. Circuits Syst. I, Reg. Papers*, vol. 64, no. 1, pp. 195–207, Jan. 2017.
[30] A. A. Modesto, F. Santos, B. Leite, and A. A. Mariano, "Linearity characterization of a multimode CMOS power amplifier for IEEE 802.11n, IEEE 802.11ax and LTE signals," in *Proc. Simpsio Sul de Microeletrnica*, May 2018.
[31] H. T. Friis, "Noise figures of radio receivers," *Proc. IRE*, vol. 32, no. 7, pp. 419–422, Jul. 1944.
[32] D. Tse and P. Viswanath, *Fundamentals of Wireless Communication*. Cambridge, U.K.: Cambridge Univ. Press, 2005.
[33] S. Cui, A. J. Goldsmith, and A. Bahai, "Energy-constrained modulation optimization," *IEEE Trans. Wireless Commun.*, vol. 4, no. 5, pp. 2349–2360, Sep. 2005.
[34] M. K. Naeem, M. Patwary, and M. Abdel-Maguid, "Universal and dynamic clustering scheme for energy constrained cooperative wireless sensor networks," *IEEE Access*, vol. 5, pp. 12318–12337, 2017.

EDSON LEONARDO DOS SANTOS received the B.S. degree in computer engineering from the Pontifical Catholic University of Paraná (PUCPR), Curitiba, Brazil, in 2012, and the M.S. degree in electrical engineering (specialization in microelectronics) from the Federal University of Paraná (UFPR), Curitiba, in 2015, where he is currently pursuing the D.S. degree in electrical engineering. He is also a Professor with the National Service of Industrial Learning (SENAI), Curitiba. Since 2013, he has participated in the development of low-power RF front-end circuits and has been a member of the Group of Integrated Circuits and Systems (GICS). His research interests include the design and modeling of energy-efficient electronic devices for wireless communication systems.

ANDRÉ AUGUSTO MARIANO received the B.S. degree in electrical engineering from the Federal University of Paraná (UFPR), Curitiba, Brazil, in 2002, the M.S. degree in microelectronics and the Ph.D. degree in electronics from the University of Bordeaux, Bordeaux, France, in 2004 and 2008, respectively. From 2004 to 2010, he was with the STMicroelectronics-IMS Joint Research Laboratory, IC Design Team. He developed a high-speed continuous-time delta–sigma A/D converter dedicated to software-defined radio and front-end receiver building blocks for millimeter-wave applications (from 60 to 77 GHz). Since February 2011, he has been an Associate Professor with the Department of Electrical Engineering, UFPR, and a member of the Group of Integrated Circuits and Systems (GICS). His research activities are focused on the design of RFICs and high-speed mixed ICs. He has several publications in journals, and international and national conferences. He holds one patent. He is also a member of the Technical Program Committees of the IEEE Latin American Symposium on Circuits and Systems (LASCAS) and the Symposium on Integrated Circuits and Systems Design (SBCCI).

GLAUBER BRANTE was born in Arapongas, Brazil, in 1983. He received the D.Sc. degree in electrical engineering from the Federal University of Technology—Paraná (UTFPR), Curitiba, Brazil, in 2013. In 2012, he was a Visiting Researcher with the Institute of Information and Communication Technologies, Electronics, and Applied Mathematics, Catholic University of Louvain, Belgium. He is currently an Assistant Professor with UTFPR. His research interests include cooperative communications, HARQ, energy efficiency, and physical layer security. He was a recipient of the Best Ph.D. Thesis Award in electrical engineering in Brazil, in 2014. He was a co-recipient of the 2016 Research Award from the Cuban Academy of Sciences. Since 2018, he has been serving as an Associate Editor for the IEEE COMMUNICATIONS LETTERS and the Co-Editor-in-Chief of the *Journal of Communication and Information Systems*.

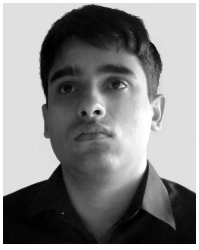

BERNARDO LEITE received the master's degree in electronics and the Ph.D. degree from the University of Bordeaux, Talence, France, in 2007 and 2011, respectively. From 2007 to 2012, he was a Researcher with the IMS Laboratory, University of Bordeaux. Since 2012, he has been an Associate Professor with the Department of Electrical Engineering, Federal University of Paraná (UFPR), Curitiba, Brazil. His research interests include the design of RF and millimeter-wave integrated circuits in silicon-based technologies, as well as the design and modeling of on-chip passive components.

RICHARD DEMO SOUZA was born in Florianópolis, Brazil. He received the B.Sc. and D.Sc. degrees in electrical engineering from the Federal University of Santa Catarina (UFSC), Brazil, in 1999 and 2003, respectively. In 2003, he was a Visiting Researcher with the Department of Electrical and Computer Engineering, University of Delaware, USA. From 2004 to 2016, he was with the Federal University of Technology—Paraná, Brazil. Since 2017, he has been with UFSC, where he is currently an Associate Professor. His research interests include the areas of wireless communications and signal processing. He is a Senior Member of the Brazilian Telecommunications Society (SBrT). He was a co-recipient of the 2014 IEEE/IFIP Wireless Days Conference Best Paper Award, the Supervisor of the awarded the Best Ph.D. Thesis in Electrical Engineering in Brazil, in 2014, and the 2016 Research Award from the Cuban Academy of Sciences. He has served as the Editor-in-Chief of the *Journal of Communication and Information Systems* (SBrT) and an Associate Editor for the IEEE COMMUNICATIONS LETTERS, *EURASIP Journal on Wireless Communications and Networking*, and IEEE TRANSACTIONS ON VEHICULAR TECHNOLOGY.

THIERRY TARIS received the master's and Ph.D. degrees from the University of Bordeaux (UB), Bordeaux, France, in 2000 and 2003, respectively. He joined the STMicroelectronics-IMS Joint Research Laboratory, UB, in 2005, as an Associate Professor, and then the Bordeaux Institute of Technology (Bx-INP), in 2014, as a Professor. He has been a member of the ST-IMS Common Laboratory for six years and an invited Senior Researcher with the Electrical and Computer Engineering Department, The University of British Columbia (UBC), Canada. He has published more than 70 papers in international journals and conferences, has ten invited papers, and is a Co-Inventor of six patents. His research interest includes the radio-frequency integrated circuits in silicon technologies. He was a recipient of three best paper awards.